Supplementary Information

1. Microstructure analysis of nanofiber

1.1. Surface roughness

The AFM of $^{e}S_7P_3$ methanol treated samples showed a slight increase in surface roughness therefore the arithmetic mean deviation was (Sa) 0.14 with standard deviation (Sq) 0.19. But $^{b}S_7P_3$ methanol treated samples showed a decrease in roughness parameters such as Sa .05 µm and Sq .07 µm. This could be due to the deformation of nanofibers after methanol treatment. However, 3D OSP measurement of $^{e}S_7P_3$ and $^{b}S_7P_3$ methanol treated samples showed to increase the roughness with arithmetic mean (Ra) 1.6 and 1.4 µm with RMS 2.2 and 1.8 µm respectively. Further contact angle showed that the surface is moderately hydrophobic, it again confirms the polymer chains functional group correlated with surface wettability.

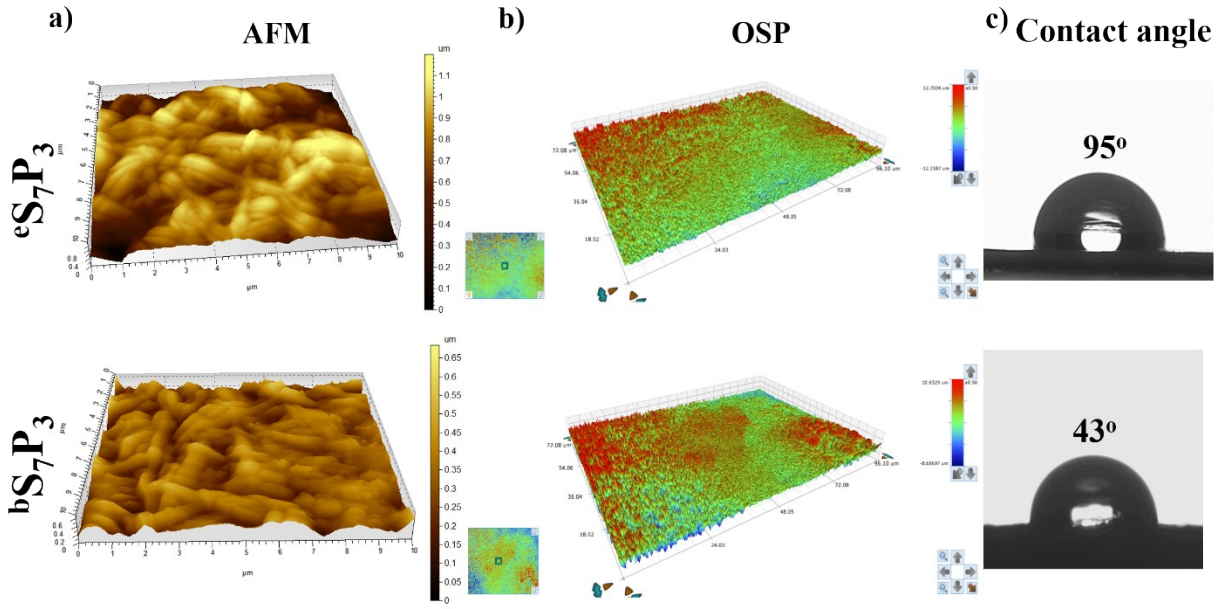

Figure 1: changes in $^{e}S_7P_3$ and $^{b}S_7P_3$ after methanol treatment a) 3D view of AFM, b) 3D view of OSP and c) static contact angle measurement

2. Physicochemical Characterization of nanofiber

2.1. ATR-FTIR

The samples were methanol treated by immersing the nanofibers samples for 15 mins for β sheet transformation of SF. Figure 2a shows the methanol treated electrospun samples ATR-FTIR

spectra. $^{e}S_5P_5$, $^{e}S_7P_3$ and $^{b}S_7P_3$ exhibited sharp peaks nearby 1624 cm^{-1} (amide I), 1518 cm^{-1} (amide II) and 1173 cm^{-1} (amide III) confirming the β sheet transformation[1]. The shift and appearance of sharp peak suggest the molecular interaction and β sheet transformation in the electrospun scaffold as a result of methanol treatment. It also confirms the presence of both the polymers with a similar extent of interaction in all the fibre compositions due to the appearance of superimposed FTIR spectra.

2.2. XRD

The exhibited diffraction peaks at 20 º for lyophilized SF sponge and PCL nanofiber with Bragg angles 2θ at 20 º, 22 º, 23 º and 28 º is enclosed in figure 2b along with XRD pattern for samples after methanol treatment. Methanol treatment confirmed the formation of β sheet transition resulted in two minor peaks at 22.6 º and 23 º for $^{e}S_5P_5$ and $^{b}S_7P_3$ respectively. The diffraction peak of $^{e}S_7P_3$ at 21.3 º further confirms the semi-crystalline structure of PCL and at 23.4 º denotes the β sheet confirmation of SF[2].

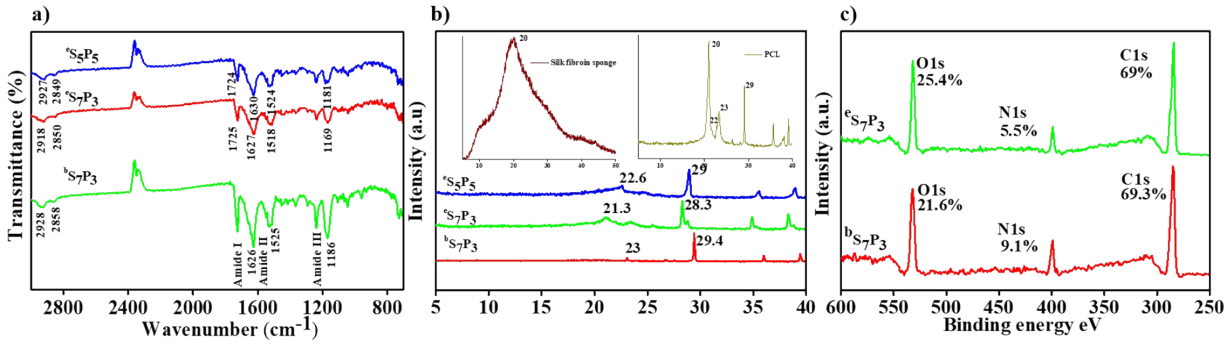

Figure 2: a) ATR-FTIR spectra, b) XRD pattern for $^{e}S_5P_5$, $^{e}S_7P_3$ and $^{b}S_7P_3$ methanol treated electrospun sheets enclosure with SF sponge and PCL fiber c) XPS spectra of $^{e}S_7P_3$ and $^{b}S_7P_3$ fiber sheets.

2.3. XPS

XPS was conducted using Instrument PHI VersaProbe III. The characterization was done on electrospun fiber samples surface. XPS analysis was performed to understand the elemental composition of electrospun fibrous samples. Figure 2c shows XPS spectra for $^{e}S_7P_3$ and $^{b}S_7P_3$ samples and their percentage elemental composition at the spot as: C1s 69 % and 69.3 %, N1s 5.5 % and 9.1% O1s 25.4 % and 21.6%. It was evident from the above analysis that there was no significant difference in elemental analysis for core-shell and monolith fibers.

2.4. Thermal Study

Differential Scanning Calorimeter (DSC) was analyzed with a temperature ranging from 5 °C to 400 °C under N_2 atmosphere with a heating rate of 10 °C/min using Perkin Elmer Pyris Diamond DSC instrument. Also, Thermo-Gravimetric and Differential Thermal Analysis (TG-DTA) was conducted with a temperature range from 30 °C to 650 °C with a heating rate of 10 °C/min using the instrument Platinum Perkin Elmer Pyris Diamond TG-DTA.

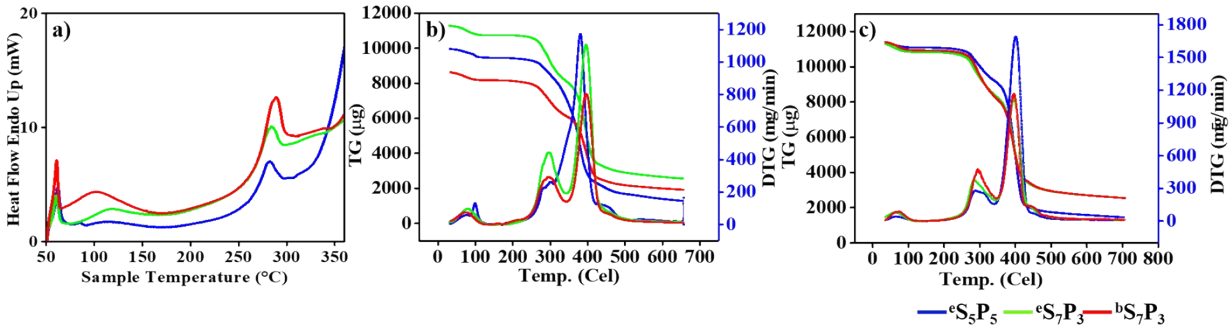

Figure 3: a) DSC curves thermogram results, b) and c) TG and DTG for $^{e}S_5P_5$, $^{e}S_7P_3$, & $^{b}S_7P_3$.

As shown in figure 4a (DSC) all three samples revealed an endothermic melting peak at around 61 °C which is consistent with the meting point of PCL. The endothermic peaks between 281 – 290 °C suggest the degradation of SF. TG-DTG curve (figure 4b & c) showed the thermal property of samples before and after methanol treatment, $^{e}S_5P_5$ has a higher DTG peak at 400 °C due to comparatively high PCL content in the sample which starts to degrade at ~360 °C[3],[4]. Interestingly $^{e}S_7P_3$ the results clearly showed high DTG peak a comparatively greater amount of weight retained in scaffold due to the property of encapsulated PCL and SF proteins retaining its complex structure. $^{b}S_7P_3$ shows a lower peak due to the interconnected composition of comparatively higher SF protein in the sample. The DTG graph of $^{b}S_7P_3$ shows a lower peak height at 280 °C compared to that of $^{e}S_7P_3$ and $^{e}S_5P_5$ samples. The degradation property of a natural polymer is slower than the synthetic therefore the curves show the degradation according to the amount of SF present in the scaffold. After methanol treatment (figure 4c) the change in the degradation curve shows the chemical composition after β sheet transformation. In $^{e}S_5P_5$ after methanol treatment did not show much difference in the DTG peak. The peak temperature and the weight loss for $^{e}S_7P_3$ and $^{b}S_7P_3$ are almost similar after methanol treatment.

References:

[1] I. C. Um, H. Y. Kweon, Y. H. Park, and S. Hudson, “Structural characteristics and properties of the regenerated silk fibroin prepared from formic acid,” *Int. J. Biol. Macromol.*, vol. 29, no. 2, pp. 91–97, Aug. 2001, doi: 10.1016/S0141-8130(01)00159-3.

[2] S. Namita, R. R. Choudhury, and N. K. Dutta, “Title: Facile and rapid ruthenium mediated photo-crosslinking of Bombyx mori silk fi broin Facile and rapid ruthenium mediated photo-crosslinking of Bombyx mori silk fibroin †,” *J. Mater. Chem. B*, no. 2, p. 6259, 2014, doi: 10.1039/c4tb00698d.

[3] J. P. Chen and Y. S. Chang, “Preparation and characterization of composite nanofibers of polycaprolactone and nanohydroxyapatite for osteogenic differentiation of mesenchymal stem cells,” *Colloids Surf. B. Biointerfaces*, vol. 86, no. 1, pp. 169–175, Aug. 2011, doi: 10.1016/J.COLSURFB.2011.03.038.

[4] A. Muñoz-Escobar, Á. de J. Ruíz-Baltazar, and S. Y. Reyes-López, “Novel Route of Synthesis of PCL-CuONPs Composites With AntimicrobialProperties,” *Dose-Response*, vol. 17, no. 3, Jul. 2019, doi: 10.1177/1559325819869502.